2-2019

L-tryptophan adsorption differentially changes the optical behaviour of pseudo-enantiomeric cysteine-functionalized quantum dots: Towards chiral fluorescent biosensors

Faezeh Askari
Department of Physics, University of Zabol

Abbas Rahdar
Department of Physics, University of Zabol

John F. Trant
Department of Chemistry and Biochemistry, University of Windsor

Sensing and Bio-Sensing Research 22 (2019) 100251

Contents lists available at ScienceDirect

Sensing and Bio-Sensing Research

journal homepage: www.elsevier.com/locate/sbsr

L-tryptophan adsorption differentially changes the optical behaviour of pseudo-enantiomeric cysteine-functionalized quantum dots: Towards chiral fluorescent biosensors

Faezeh Askari[a], Abbas Rahdar[a,*], John F. Trant[b,*]

[a] Department of Physics, University of Zabol, Zabol, P. O. Box. 35856-98613, Islamic Republic of Iran
[b] Department of Chemistry and Biochemistry, University of Windsor, Windsor, ON N9B 3P4, Canada

ARTICLE INFO

Keywords:
Graphene quantum dots
Click chemistry
Chiral sensors
Circular dichroism
Fluorescence

ABSTRACT

Water-soluble chiral graphene quantum dots (GQDs) with a strong blue emission were synthesized by covalently immobilizing L-cysteine or D-cysteine onto the GQDs. Either the amine or the thiol group of cysteine was used to make the bond through amide coupling or thiol-ene click chemistry respectively. The functionalized chiral GQDs were the characterized by FT-IR and UV–vis. The enantiomeric pairs exhibit equal but opposite bands in circular dichroism spectra suggesting that there is no difference in the efficacy of conjugation. The fluorescent response of these chiral GQDs when exposed to L-tryptophan was then studied. The fluorescence of the amide-conjugated GQDs was quenched with the addition of L-Trp regardless of which enantiomer of cysteine was present on the surface. The thiol-linked D- Cys GQDs fluorescence was also quenched on exposure to L-Trp, but the fluorescence of the thiol-linked L-Cys GQDs was unaffected under the same conditions.

1. Introduction

Graphene quantum dots (GQDs), with intriguing optical behaviour due to quantum confinement effects [1–3], have potential applications as light emitting devices, bioassay tools, bioimaging probes, drug delivery vehicles, and fluorescent sensors. Their good biocompatibility, high stability [4], and most importantly, high quantum yields (which allows for very low loading, provide them with an advantage over other fluorescent dye systems [5]. However, in almost any biological application, chirality must be considered, and the development of chiral quantum dots remains a challenge. There are still only limited studies focusing on the chiral properties of GQDs [6–10], and to the best of our knowledge no reports using chiral GQDs as fluorescent sensors have been reported, although there are a number of reports of conductance sensors based on GQDs [11–13]. Instead, much of the focus relating to chiral quantum dots has focused on their semiconducting properties and looking to use changes in conductance as a measurement of analyte [14–17]. However, toxicity, loading, and poor solubility of these dots has limited their application. Simpler systems that use fluorescence as the read-out may provide a fruitful avenue of research [13].

Although enantiomeric GQDs have identical fluorescent behaviour, diastereomeric complexes formed with analytes in their environment can differentially affect fluorescence due to differences in the energy transfer occurring at the surface [18]. This means that a chiral GQD surface can potentially act as a fluorescent sensor to detect one enantiomer of a given molecule such as a small molecule drug, nucleic acid, or amino acid. This principle has been exploited in many other systems and is appropriate for GQDs [19–21].

Due to its fluorescence, tryptophan is an ideal model analyte. The presence of tryptophan in food samples can be used to help identify origin of the food and to detect tampering [22]. The importance of Trp in serotonin and niacin biosynthesis makes the detection of Trp an important consideration [23]. Consequently, there has been some effort into quantifying the amount of tryptophan present in a given sample [24–26]. Additional detection techniques would be useful, and employing GQDs as colored fluorescent sensors would require less material, use only simple instrumentation, and would not require access to additional special reagents. This has been noted by others, and there are several reports employing functionalized GQDs for the detection of tryptophan; however, the approaches are electrochemical in nature [11,12,27–30], or have employed host-guest chemistry with the inherent complexities involved in the conjugation [31]. A simple chiral molecule covalently immobilized on the GQD surface with a fluorescent read-out would be of interest.

We wish to disclose our investigations into using cysteine-functionalized GQDs to provide a fluorescent probe for Trp. *N*-acetyl cysteine

* Corresponding authors.
E-mail addresses: a.rahdar@uoz.ac.ir (A. Rahdar), j.trant@uwindsor.ca (J.F. Trant).

https://doi.org/10.1016/j.sbsr.2018.100251
Received 27 October 2018; Received in revised form 3 December 2018; Accepted 4 December 2018

has been used with traditional CdSe/CdS quantum dots to differentiate between different enantiomers of tyrosine [32]. In that case the *N*-acetylcysteine was absorbed onto the surface of the dots under alkaline conditions forcing the carboxyl group and thiol to be affixed to the surface. However, with tryptophan, we believe the key interaction may involve the carboxylate as a hydrogen-bond acceptor, and either the thiol or amino-hydrogens as hydrogen-bond donors. Either system-free amine or free thiol- can be accessed by using the other functionality to conjugate the amino acid to the GQD. An argument can be made for both ligation techniques and for why the chiral discrimination of either option might be preferred. Consequently, we wished to investigate both a thiol-bound and an amino-bound version of our chiral GQD and determine their potential as chiral fluorescent probes for L-tryptophan.

2. Experimental section

2.1. Reagents

Citric acid, sodium hydroxide, sodium dihydrogen phosphate, disodium hydrogen phosphate, ammonium persulfate, sodium borohydride, L-tryptophan, and L-cysteine HCl were purchased from Merck. N-(3-Dimethylaminopropyl)-N′-ethylcarbodiimide hydrochloride (EDC) was purchased from Bio Basic. Sulfo-N-hydroxysuccinimide (S-NHS) was purchased from Sigma–Aldrich. D-cysteine was purchased from EXIR. Doubly distilled water was used throughout the experiment.

2.2. Synthesis of graphene quantum dots (GQDs)

The GQDs were synthesized by pyrolyzing carbon precursors [33]. 1 g of citric acid was put into a pyrex glass beaker and heated to 200 °C using a hotplate (Corning). After 5 min, the citric acid had melted, and the liquid had turned yellow. After further heating for an additional 10 min, the liquid turned orange, indicative of the formation of GQDs. The beaker was immediately removed from the heat source and allowed to cool. After reaching ambient temperature, the solution was adjusted to pH 7 using 1 M NaOH solution (12 mL) providing a solution of GQDs in water. The solution (approx. 12 mL) was then dialyzed against 20 mL DI water using 3.5 kDa cut-off dialysis tubing (Spectrum Labs) for 24 h. The dialysate in the beaker, containing the GQDs, was collected and put aside. The reaction solution in the dialysis tube was then dialysed against an additional fresh 20 mL of DI water for 24 h. The dialysis tubing and its contents was then discarded. The combined dialysates were then dialysed against 100 mL of DI water in a 1.0 kDa cut-off dialysis tubing to remove any residual citric acid. The contents of the tube, the GQDs, were then lyophilized and stored as a powder at −20 °C until needed.

2.2.1. Amide coupling of L-cysteine or D-cysteine to the GQDs

0.1 g of dried GQDs powder as limiting reagent was first dissolved in 1 mL of sodium phosphate buffer (Dissolve 1.09 g of Na_2HPO_4 and 0.31 g of NaH_2PO_4 in 100 mL of H_2O) at pH 7.4. A solution of EDC in this buffer (0.116 g, 3 mL) was added to the suspended GQDs with magnetic stirring. After 15 min of stirring, S-NHS (0.07 g, 3 mL) was added to the above solution and the reaction mixture was stirred for an additional 30 min. Finally, either L-cysteine•HCl (0.118 g, 3 mL) or D-cysteine (0.09 g, 3 mL) was added to the reaction mixture and the solution was allowed to stir, in the dark, for 24 h. The resulting mixtures were then dialyzed using 1 kDa cut-off dialysis tubing (Spectrum Labs) against either DI water (2 × 12 h) to provide samples for analysis or against PBS buffer for the binding assays (then diluted to 40 mL). In the former case, the samples were lyophilized, in the latter, they were left in solution and stored at 4 °C until needed. This provided a 2.5 mg/mL solution of GQDs.

2.2.2. Thiol-ene conjugation of L-cysteine or D-cysteine to the GQDs

GQD powder was resuspended in ethanol (20 mg in 10 mL) and a large excess of sodium borohydride (50 mg) was added to reduce the carbonyl groups on the surface [34]. The reaction was considered complete when no additional hydrogen bubbles had been observed for 5 min (20 min total). The GQDs were then dialyzed twice against DI water, 1 kDa cutoff (100 mL. water) and lyophilized to provide 20 mg of material. This reduced GQD (50 mg) was resuspended in DI water, and ammonium persulfate (2.5 g, 0.01 mmol) was added to the flask with magnetic stirring [35]. The flask was wrapped in aluminium foil, and heated at 90 °C for 1 h. Then either L-cysteine•HCl (86 mg, 0.99 mmol) or D-cysteine (60 mg, 0.99 mmol) was added and the mixture, diluted to a total volume of 20 mL of water, was refluxed for an additional 24 h. After cooling, the solution was dialyzed three times against 200 mL of DI water in 1 kDa cut-off dialysis tubing. This provided a 2.5 mg/mL solution of GQDs.

2.3. Fluorescent assay for the optical effects of L-tryptophan interaction with amide-linked GQDs (L_{Cys}-GQDs; D_{Cys}-GQDs)

An aqueous solution of L-tryptophan (80 mM) was prepared. 20 μL of the L_{Cys}-GQDs or D_{Cys}-GQDs was added to 2 mL of PBS, and the entire solution was transferred to a quartz cuvette. Then aliquots of the L-tryptophan solution were added to the cuvette with pipette mixing and the fluorescence spectrum of the mixture was recorded after each addition using an excitation wavelength of 300 nm.

2.4. Fluorescent assay for the optical effects of L-tryptophan interaction with thiol-linked GQDs (L_{Cys}- clicked GQDs; D_{Cys}- clicked GQDs)

An aqueous solution of L-tryptophan (80 mM) was prepared. 5 μL of the L_{Cys}-clicked GQDs or D_{Cys}-clicked GQDs was added to 2 mL of PBS, and the entire solution was transferred to a quartz cuvette. Then aliquots of the L-tryptophan solution were added to the cuvette with pipette mixing and the fluorescence spectrum of the mixture was recorded after each addition using an excitation wavelength of 360 nm.

2.5. Characterization

Fourier transform infrared (FTIR) spectra were acquired by preparing KBr discs with the analyte, and measuring the spectra using a Perkin-Elmer Spectrum RXI FT-IR spectrophotometer. UV–Vis absorption spectra were recorded using a Perkin Elmer Lambda 25 UV/Vis spectrophotometer. All fluorescent spectra were taken with a Jasco FP8500 spectrophotometer. AFM images were obtained using the non-contact mode using an ARA-AFM (ARA, Iran). Droplets of the GQD solutions (40 μL) were deposited on the surface of freshly prepared mica. After drying the AFM image was recorded. High-resolution transmission electron microscopy (HR-TEM) images were recorded on a Jeol, JEM-2100F operating at 200 kV. The circular dichroism spectra measurement was recorded on a circular dichroism spectrometer (model 215, Aviv, USA). Circular dichroism nerve network (CDNN) software was utilized for data analysis. All optical measurements were carried out in quartz cuvettes at ambient temperature.

3. Results and discussion

3.1. Synthesis

The carboxylic acid functionality of the cysteine is expected to be important for diastereomeric complex formation as the hydrogen bond acceptor. However, an argument can be made for using either the thiol or the amino-group as the hydrogen bond donor. This means either

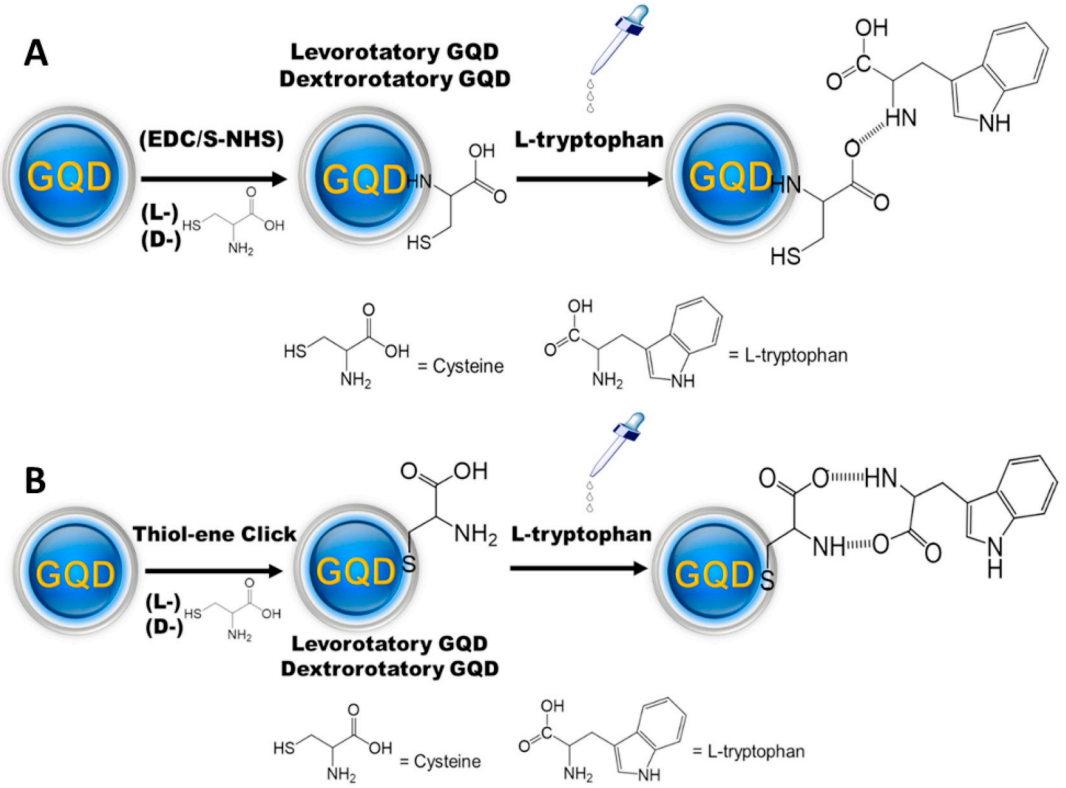

Fig. 1. a) Synthesis of amide-conjugated chiral cysteine-functionalized GQDs (L_{cys}-GQDs and D_{cys}-GQDs) and a schematic representation of the expected interactions with L-tryptophan. b) Synthesis of thiol-conjugated chiral cysteine-functionalized GQDs (L_{cys}-clicked GQDs and D_{cys}-clicked GQDs) and a schematic representation of the expected interactions with L-tryptophan.

functionality can be used to immobilize the amino acid on the surface of the particle. This provides options for the synthesis. An amide bond can be used to immobilize the cysteine on the surface as the GQD surface, derived from citric acid, is rich in carboxylic acid functionalities (Fig. 1a). However, direct coupling of cysteine would require the carboxylic acid on the amino acid to be protected to avoid homocoupling. This would involve unnecessary chemical manipulation of functionalized GQDs. Consequently, we used a two-step *in situ* protocol activating the GQDs with S-NHS, with EDC as coupling agent to introduce an activated handle, and then treating these electrophilic GQDs with either enantiomer of cysteine to make either of the pseudo-enantiomeric GQDs. These would be expected to interact with tryptophan primarily through only the carboxylic acid moiety.

Alternatively, the cysteine could be immobilized through the thiol functionality, allowing for both the amine and the carboxylic acid moieties to be involved in the organization of the tryptophan (Fig. 1b). This would be expected to provide a more organized diastereomeric complex. We hypothesized that this would be more likely to induce differential fluorescent behaviour in our GQDs than the amine-conjugated system. Cysteine has been immobilized onto quantum dots through sulfur before [15,36], but normally by invoking strong cysteine-transition metal bonds. A carbon-rich surface does not allow for this possibility. Instead, we identified that a thiol-ene "click" reaction [37] would allow for the easy chemoselective immobilization of the cysteine. The carbonyl functionalities on the surface of the GQDs were converted to olefins using a two-step protocol: reduction with sodium borohydride followed by elimination using ammonium persulfate. Cysteine (either enantiomer) was then added, and the thiol-ene click reaction was carried out to provide the L_{cys}-clicked GQDs or D_{cys}-clicked GQDs.

3.2. Characterization of the GQDs

The labelled GQDs were then characterized using high-resolution transmission electron microscopy (HR-TEM) and atomic force microscopy (AFM). Representative images are provided as Fig. 2. The diameter of GQDs are less than 5 nm, and the average size of the GQDs was calculated to be about 2.9 nm. Similar HR-TEM images of GQDs are well precedented in the literature, and they are indicated by the clusters of parallel lines [38–42]. The AFM results support the HR-TEM images as they imply that the GQD size distribution is on the order of 0.2–2 nm. The good agreement of these two independent measurements provides confidence for demonstrating the successful synthesis of the GQDs.

Circular Dichroism (CD) measurements were used to confirm that pseudo-enantiomeric optically-active GQDs were generated by conjugation to either L-cysteine or D-cysteine (Fig. 3). Both the amine-linked (Fig. 3a) and the thiol-linked systems (Fig. 3b) show pseudo-symmetry as expected. We ensured that the degree of functionalization was comparable by measuring the absorbance spectra of both systems (insets in Fig. 3). Together these spectra indicate that pseudo-enantiomers were indeed prepared. The CD spectra for the two systems is of course different as the mode of conjugation is different. Similarly, the spectra are not reflections in the x-axis as the GQDs will of course influence the orientation of the cysteine ligands, this same phenomenon has been previously observed by others [6].

The CD spectra support the presence of a chiral environment but do not indicate the origins of the chirality, although it must be derived from the presence of the chiral cysteine residues on the surface of the nanoparticles. FT-IR analysis is a simple technique that allowed us to confirm the presence of the expected functionalities (Fig. 4). The most pronounced IR absorption bands in the native GQDs occur at

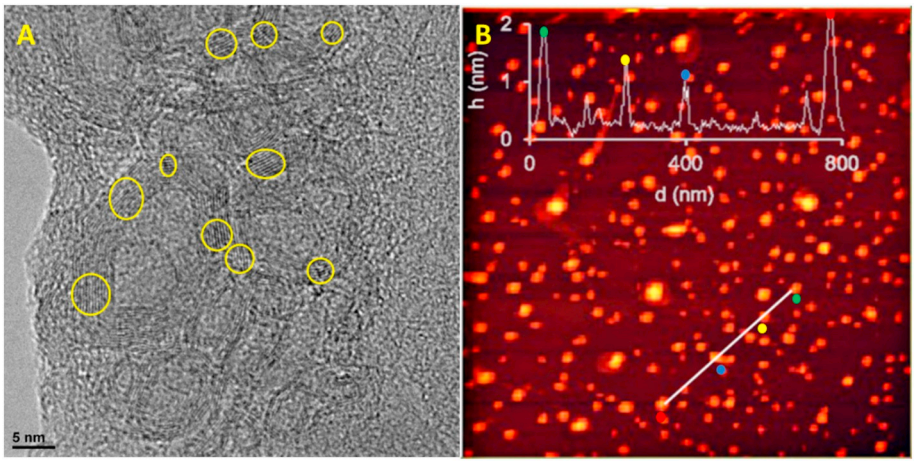

Fig. 2. A) HR-TEM image of the GQDs. The particles have an average diameter of 2.9 nm and can be identified by the parallel line structures. Some are highlighted with the yellow circles. B) AFM image of GQDs on mica substrates with the height profile along the line in the image. The field of view of the AFM image is 2.0 μm × 2.0 μm. Both images are of the unmodified GDQs. (For interpretation of the references to colour in this figure legend, the reader is referred to the web version of this article.)

3427 cm^{-1} (νOH from the COOH groups), 1582 cm^{-1} (νC = O), 1390 cm^{-1} (νsCOO), and 1255 cm^{-1} (νC–O). (Fig4a, blue line). FT-IR spectra of GQDs (Fig. 4a, blue line) show strong absorption peaks for carboxyl groups. Coupling to the amines is expected to cap many of these acids. The relative amplitude of the 3427 cm^{-1} peak decreases, with a concomitant appearance of new vibrations in the range of 2670–2550 cm^{-1} indicative of S—H vibrations [43]. The new strong carbonyl frequencies at 1699 cm^{-1} and 1580 cm^{-1} are a result of the amide absorption modes and are typically used to identify the success of amide-bond formation on the surface of nanoparticles [44,45]. The two pseudo-enantiomers provide similar spectra as expected, offset only by moderate changes in amplitude due to slightly different sample amounts. We also used FT-IR to confirm the success of the thiol-ene chemistry for the other series of GQDs. No thiol peaks are observable, neither are there any new amide peaks. Instead there are new signals at 3539 cm^{-1} that are consistent with the presence of amine N—H stretches [36].

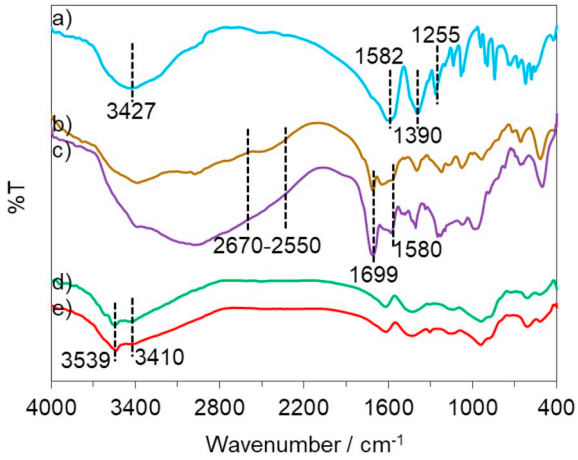

Fig. 4. FT-IR spectra of unmodified GQDs (a); amine-linked L_{Cys}- GQDs (b), D_{Cys}- GQDs (c); and thiol-linked L_{Cys}- clicked GQDs (d) and D_{Cys}- clicked GQDs (e). Spectra are offset vertically to simplify the image, % transmittance is relative within a spectrum.

3.3. Fluorescence studies

With the cysteine immobilization confirmed, we examined the fluorescence behavior of the cysteine-modified GQDs in the presence of tryptophan. Tryptophan is an excellent model compound for these analyses as it is inherently fluorescent and its spectrum is highly dependent on the solvation environment [46]. Interaction with the surface cysteines can be expected to influence the fluorescence of the GQDs [47,48]. We began by investigating the interaction with the amine-conjugated L_{cys}-GQDs and D_{cys}-GQDs. In this system, the carboxylate and the thiol hydrogen could potentially form an eleven-

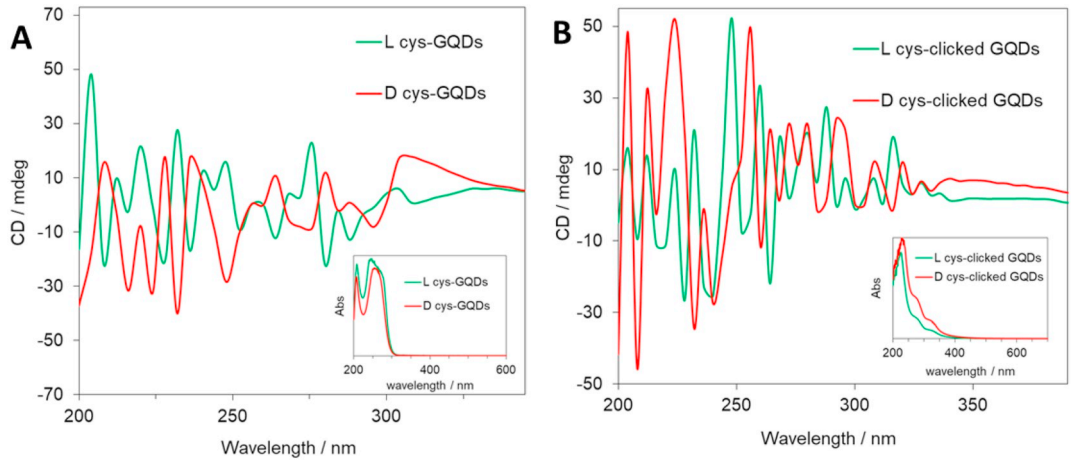

Fig. 3. CD spectra of cysteine-functionalized GQDs. Panel A shows the amide-linked systems, while panel B provides the spectra of the thiol-ene conjugated systems. Green lines represent the L-cysteine samples and red lines the D-cysteine samples. Samples were measured at a concentration of 2.5 mg/mL using a quartz cuvette with a 1 cm path length. The same samples in the same cuvettes were analyzed using UV–Vis spectroscopy (insets). (For interpretation of the references to colour in this figure legend, the reader is referred to the web version of this article.)

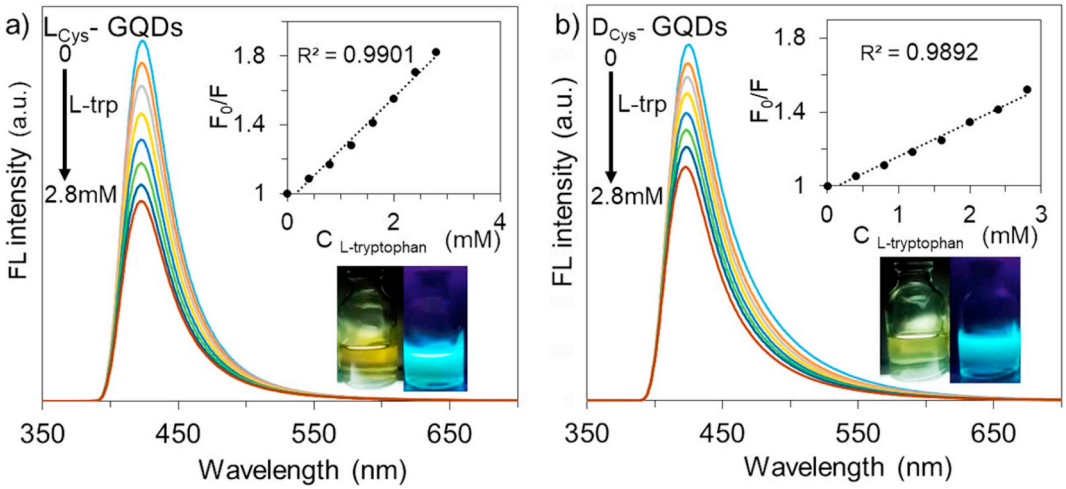

Fig. 5. The fluorescence spectra of the tryptophan titration studies of a) L_{Cys}-GQDs and b) D_{Cys}-GQDs. Insets: (upper) Stern-Volmer plots of the quenching interactions between the GQDs and L-Trp; (lower) Photographs of the final solutions acquired under either visible light (left) or under UV light (right) show that fluorescence is maintained as blue emission. (For interpretation of the references to colour in this figure legend, the reader is referred to the web version of this article.)

membered ring with the tryptophan or interact through an open-chain form. An excitation wavelength of 300 nm, near the λ_{max} was chosen for the L_{Cys}-GQDs and D_{Cys}-GQDs. Tryptophan was then titrated into the cuvette and the spectra acquired after each addition (Fig. 5).

The fluorescence intensity of both L_{Cys}-GQDs and D_{Cys}-GQDs decreased upon increasing the L-Trp concentration from 0 to 2.8 mM. A change in fluorescence is expected as the optical behaviour of quantum dots is affected by their surface functionalization, and the formation of cysteine-tryptophan complexes would be expected to shift the amplitude, or even the wavelength, of the emission spectrum through quenching: small changes in surface functionalization change amplitude of emission [49]. Linear Stern–Volmer relationships were observed for the interaction in the L-Trp mM range (F_0/F *versus* L-trp). The lifetime of the emissive state of the pseudo-enantiomeric GQDs should be identical so the difference in slope can be attributed to a difference in the quencher rate co-efficient [50]. The quenching constants are 0.30 mM^{-1} and 0.19 mM^{-1} for the two systems respectively: there is clearly some discrimination between pseudo-diastereomeric complexes, but it is not sufficient to be useful. The diastereomeric complex, if it does form an eleven membered ring or simply an open chain form, is potentially too disorganized to induce a significant differentiation in the fluorescence profile of the GQDs.

On the other hand, the thiol-ene functionalized GQDs will allow for the formation of a smaller 10-membered ring and would use an amine in place of a thiol as the solid-supported hydrogen-bond donor. We examined the fluorescent response of these systems (L_{cys}-clicked GQDs and D_{cys}-clicked GQDs) to tryptophan titration using an excitation wavelength of 360 nm (Fig. 6).

These systems clearly behave differently. The D_{Cys}-clicked GQDs are quenched in a dose-dependent manner by tryptophan; however, the amplitude of the fluorescence of the L_{Cys}-clicked GQDs are completely unaffected, although there is a slight red shift as the tryptophan concentration increases. A slope 0 line in the Stern-Volmer plot of the L_{Cys}-clicked GQDs indicates that there is no quenching (the quencher rate co-efficient is 0), while the D_{Cys}-clicked GQDs show a positive value (although smaller than that observed for the amine-linked systems above, 0.058 mM^{-1}). The data indicates that L-tryptophan does not interact with L-cysteine on the surface of the GQDs, but does interact with D-cysteine. The result is empirical, and more work needs to be done to explain this selectivity.

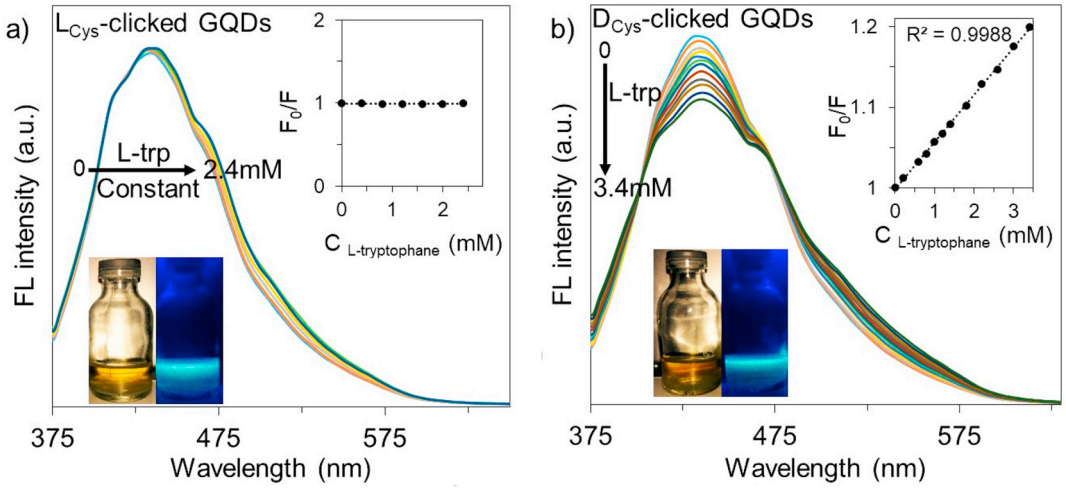

Fig. 6. The fluorescence spectra of the tryptophan titration studies of a) L_{Cys}-clicked GQDs and b) D_{Cys}-clicked GQDs. Insets: (upper) Stern-Volmer plots of the quenching interactions between the GQDs and L-Trp; (lower) Photographs of the final solutions acquired under either visible light (left) or under UV light (right) show that fluorescence is maintained as blue emission. (For interpretation of the references to colour in this figure legend, the reader is referred to the web version of this article.)

4. Conclusion

Chiral GQDs were prepared by conjugating either enantiomer of cysteine to GQDs using either amine coupling or thiol-ene click chemistry. The chiral GQDs were characterized by AFM, HR-TEM, CD-spectroscopy, UV–Vis absorbance and FT-IR. All four systems were evaluated as potential fluorescent sensors for L-tryptophan. Both amine-conjugated systems showed a similar dose-responsive quenching to the presence of L-tryptophan, as did the D-cysteine thiol-ene clicked GQDs. The L-cysteine thiol-ene clicked GQDs, however, demonstrated no change to the fluorescent signal with increasing tryptophan concentrations. Consequently, a twinned assay using the pseudoenatiomeric thiol-ene clicked cysteine GQDs can act as chiral sensors to detect L-tryptophan. These GQDs provide a proof-of-concept that chiral GQDs can act as chiral fluorescent sensors and could form the basis for the development of chiral quantum dots with potential applications in biomedicine.

Conflict of interest

The authors declare no conflicts of interest.

Acknowledgments

The Authors would like to thank the University of Zabol for financial support for this work. This work was funded by the Natural Sciences and Engineering Research Council of Canada grant # 2018-06338 to JFT.

References

[1] R. Wang, K.-Q. Lu, Z.-R. Tang, Y.-J. Xu, Recent progress in carbon quantum dots: synthesis, properties and applications in photocatalysis, J. Mater. Chem. A 5 (2017) 3717–3734, https://doi.org/10.1039/c6ta08660h.
[2] Y. Wang, A. Hu, Carbon quantum dots: synthesis, properties and applications, J. Mater. Chem. C 2 (2014) 6921–6939, https://doi.org/10.1039/c4tc00988f.
[3] Y. Shirasaki, G.J. Supran, M.G. Bawendi, V. Bulović, Emergence of colloidal quantum-dot light-emitting technologies, Nat. Photonics 7 (2012) 13, https://doi.org/10.1038/nphoton.2012.328.
[4] L. Fan, Y. Hu, X. Wang, L. Zhang, F. Li, D. Han, Z. Li, Q. Zhang, Z. Wang, L. Niu, Fluorescence resonance energy transfer quenching at the surface of graphene quantum dots for ultrasensitive detection of TNT, Talanta 101 (2012) 192–197, https://doi.org/10.1016/j.talanta.2012.08.048.
[5] Z.L. Wu, M.X. Gao, T.T. Wang, X.Y. Wan, L.L. Zheng, C.Z. Huang, A general quantitative pH sensor developed with dicyandiamide N-doped high quantum yield graphene quantum dots, Nanoscale 6 (2014) 3868–3874, https://doi.org/10.1039/c3nr06353d.
[6] N. Suzuki, Y. Wang, P. Elvati, Z.-B. Qu, K. Kim, S. Jiang, E. Baumeister, J. Lee, B. Yeom, J.H. Bahng, J. Lee, A. Violi, N.A. Kotov, Chiral graphene quantum dots, ACS Nano 10 (2016) 1744–1755, https://doi.org/10.1021/acsnano.5b06369.
[7] M. Vázquez-Nakagawa, L. Rodríguez-Pérez, M.A. Herranz, N. Martín, Chirality transfer from graphene quantum dots, Chem. Commun. 52 (2016) 665–668, https://doi.org/10.1039/c5cc08890a.
[8] Y. Zhang, L. Hu, Y. Sun, C. Zhu, R. Li, N. Liu, H. Huang, Y. Liu, C. Huang, Z. Kang, One-step synthesis of chiral carbon quantum dots and their enantioselective recognition, RSC Adv. 6 (2016) 59956–59960, https://doi.org/10.1039/c6ra12420h.
[9] X. Zhao, J. Gao, X. He, L. Cong, H. Zhao, X. Li, F. Tan, DNA-modified graphene quantum dots as a sensing platform for detection of Hg2 + in living cells, RSC Adv. 5 (2015) 39587–39591, https://doi.org/10.1039/C5RA06984J.
[10] P.G. Luo, F. Yang, S.-T. Yang, S.K. Sonkar, L. Yang, J.J. Broglie, Y. Liu, Y.-P. Sun, Carbon-based quantum dots for fluorescence imaging of cells and tissues, RSC Adv. 4 (2014) 10791–10807, https://doi.org/10.1039/c3ra47683a.
[11] Y. Yu, W. Liu, J. Ma, Y. Tao, Y. Qin, Y. Kong, An efficient chiral sensing platform based on graphene quantum dot-tartaric acid hybrids, RSC Adv. 6 (2016) 84127–84132, https://doi.org/10.1039/c6ra18477d.
[12] Q. Xiao, S. Lu, C. Huang, W. Su, S. Zhou, J. Sheng, S. Huang, An electrochemical chiral sensor based on amino-functionalized graphene quantum dots/β-cyclodextrin modified glassy carbon electrode for enantioselective detection of tryptophan isomers, J. Iran. Chem. Soc. 14 (2017) 1957–1970, https://doi.org/10.1007/s13738-017-1134-9.
[13] E. Zor, E. Morales-Narváez, A. Zamora-Gálvez, H. Bingol, M. Ersoz, A. Merkoçi, Graphene Quantum Dots-based Photoluminescent Sensor: a Multifunctional Composite for Pesticide Detection, ACS Appl. Mater. Interfaces 7 (2015) 20272–20279, https://doi.org/10.1021/acsami.5b05838.
[14] M.P. Moloney, Y.K. Gun'ko, J.M. Kelly, Chiral highly luminescent CdS quantum dots, Chem. Commun. (2007) 3900–3902, https://doi.org/10.1039/b704636g.
[15] C. Carrillo-Carrión, S. Cárdenas, B.M. Simonet, M. Valcárcel, Selective quantification of carnitine enantiomers using chiral cysteine-capped CdSe(ZnS) quantum dots, Anal. Chem. 81 (2009) 4730–4733, https://doi.org/10.1021/ac900034h.
[16] T. Nakashima, Y. Kobayashi, T. Kawai, Optical activity and Chiral memory of Thiol-Capped CdTe Nanocrystals, J. Am. Chem. Soc. 131 (2009) 10342–10343, https://doi.org/10.1021/ja902800f.
[17] C. Han, H. Li, Chiral Recognition of Amino Acids based on Cyclodextrin-Capped Quantum Dots, Small 4 (2008) 1344–1350, https://doi.org/10.1002/smll.200701221.
[18] M.J. Deka, D. Chowdhury, Chiral carbon dots and their effect on the optical properties of photosensitizers, RSC Adv. 7 (2017) 53057–53063, https://doi.org/10.1039/c7ra10611d.
[19] L. Pu, Enantioselective fluorescent sensors: a tale of BINOL, Acc. Chem. Res. 45 (2012) 150–163, https://doi.org/10.1021/ar200048d.
[20] T. Ikai, N. Nagata, S. Awata, Y. Wada, K. Maeda, M. Mizuno, T.M. Swager, Optically active distorted cyclic triptycenes: chiral stationary phases for HPLC, RSC Adv. 8 (2018) 20483–20487, https://doi.org/10.1039/c8ra04434a.
[21] J.R. Lakowicz, Quenching of fluorescence, Principles of Fluorescence Spectroscopy, Springer US, Boston, MA, 2006, pp. 277–330.
[22] V.M. Wheatley, J. Spink, Defining the Public Health Threat of Dietary Supplement Fraud, Compr. Rev. Food Sci. Food Saf. 12 (2013) 599–613, https://doi.org/10.1111/1541-4337.12033.
[23] T. Fukuwatari, K. Shibata, Nutritional aspect of tryptophan metabolism, Int. J. Tryp. Res. 6 (2013) 3–8, https://doi.org/10.4137/ijtr.s11588.
[24] S. Mustafa, W. Hashim, S. Khaliq, R.A. Khan Azizuddin, An improved high performance liquid chromatographic method for tryptophan analysis in rat brain administrated by seaweed, J. Anal. Bioanal. Tech. 5 (2014) 1000188, https://doi.org/10.4172/2155-9872.1000188.
[25] J. Ren, M. Zhao, J. Wang, C. Cui, B. Yang, Spectrophotometric method for determination of tryptophan in protein hydrolysates, Food Technol. Biotechnol. 45 (2007) 360–366 http://hrcak.srce.hr/file/36388.
[26] S. Dziomba, A. Bekasiewicz, A. Prahl, T. Bączek, P. Kowalski, Improvement of derivatized amino acid detection sensitivity in micellar electrokinetic capillary chromatography by means of acid-induced pH-mediated stacking technique, Anal. Bioanal. Chem. 406 (2014) 6713–6721, https://doi.org/10.1007/s00216-014-8104-1.
[27] L. Guo, L. Bao, B. Yang, Y. Tao, H. Mao, Y. Kong, Electrochemical recognition of tryptophan enantiomers using self-assembled diphenylalanine structures induced by graphene quantum dots, chitosan and CTAB, Electrochem. Commun. 83 (2017) 61–66, https://doi.org/10.1016/j.elecom.2017.08.024.
[28] J. Ou, Y. Tao, J. Xue, Y. Kong, J. Dai, L. Deng, Electrochemical enantiorecognition of tryptophan enantiomers based on graphene quantum dots–chitosan composite film, Electrochem. Commun. 57 (2015) 5–9, https://doi.org/10.1016/j.elecom.2015.04.004.
[29] J. Ou, Y. Zhu, Y. Kong, J. Ma, Graphene quantum dots/β-cyclodextrin nanocomposites: a novel electrochemical chiral interface for tryptophan isomer recognition, Electrochem. Commun. 60 (2015) 60–63, https://doi.org/10.1016/j.elecom.2015.08.005.
[30] D. Guo, Y. Huang, C. Chen, Y. Chen, Y. Fu, A sensing interface for recognition of tryptophan enantiomers based on porous cluster-like nanocomposite films, New J. Chem. 38 (2014) 5880–5885, https://doi.org/10.1039/c4nj01484g.
[31] Y. Wei, H. Li, H. Hao, Y. Chen, C. Dong, G. Wang, β-Cyclodextrin functionalized Mn-doped ZnS quantum dots for the chiral sensing of tryptophan enantiomers, Polym. Chem. 6 (2015) 591–598, https://doi.org/10.1039/c4py00618f.
[32] F. Gao, S. Ma, X. Xiao, Y. Hu, D. Zhao, Z. He, Sensing tyrosine enantiomers by using chiral CdSe/CdS quantum dots capped with N-acetyl-L-cysteine, Talanta 163 (2017) 102–110, https://doi.org/10.1016/j.talanta.2016.10.091.
[33] S. Wang, Z.-G. Chen, I. Cole, Q. Li, Structural evolution of graphene quantum dots during thermal decomposition of citric acid and the corresponding photoluminescence, Carbon 82 (2015) 304–313, https://doi.org/10.1016/j.carbon.2014.10.075.
[34] W. Zhang, Y. Liu, X. Meng, T. Ding, Y. Xu, H. Xu, Y. Ren, B. Liu, J. Huang, J. Yang, X. Fang, Graphenol defects induced blue emission enhancement in chemically reduced graphene quantum dots, Phys. Chem. Chem. Phys. 17 (2015) 22361–22366, https://doi.org/10.1039/c5cp03434e.
[35] E.K. Skinner, F.M. Whiffin, G.J. Price, Room temperature sonochemical initiation of thiol-ene reactions, Chem. Commun. 48 (2012) 6800–6802, https://doi.org/10.1039/c2cc32457a.
[36] J. Chen, Y. Gao, Z. Xu, G. Wu, Y. Chen, C. Zhu, A novel fluorescent array for mercury (II) ion in aqueous solution with functionalized cadmium selenide nanoclusters, Anal. Chim. Acta 577 (2006) 77–84, https://doi.org/10.1016/j.aca.2006.06.039.
[37] A.B. Lowe, Thiol-ene "Click" reactions and recent applications in polymer and materials synthesis: a first update, Polym. Chem. 5 (2014) 4820–4870, https://doi.org/10.1039/c4py00339j.
[38] Y. Dong, J. Shao, C. Chen, H. Li, R. Wang, Y. Chi, X. Lin, G. Chen, Blue luminescent graphene quantum dots and graphene oxide prepared by tuning the carbonization degree of citric acid, Carbon 50 (2012) 4738–4743, https://doi.org/10.1016/j.carbon.2012.06.002.
[39] S. Sahu, B. Behera, T.K. Maiti, S. Mohapatra, Simple one-step synthesis of highly luminescent carbon dots from orange juice: application as excellent bio-imaging agents, Chem. Commun. 48 (2012) 8835–8837, https://doi.org/10.1039/c2cc33796g.
[40] L. Tang, R. Ji, X. Cao, J. Lin, H. Jiang, X. Li, K.S. Teng, C.M. Luk, S. Zeng, J. Hao, S.P. Lau, Deep Ultraviolet Photoluminescence of Water-Soluble Self-Passivated Graphene Quantum Dots, ACS Nano 6 (2012) 5102–5110, https://doi.org/10.

1021/nn300760g.
[41] H. Zhang, H. Huang, H. Ming, H. Li, L. Zhang, Y. Liu, Z. Kang, Carbon quantum dots/Ag3PO4 complex photocatalysts with enhanced photocatalytic activity and stability under visible light, J. Mater. Chem. 22 (2012) 10501–10506, https://doi.org/10.1039/c2jm30703k.
[42] H. Ming, Z. Ma, Y. Liu, K. Pan, H. Yu, F. Wang, Z. Kang, Large scale electrochemical synthesis of high quality carbon nanodots and their photocatalytic property, Dalton Trans. 41 (2012) 9526–9531, https://doi.org/10.1039/c2dt30985h.
[43] M. Koneswaran, R. Narayanaswamy, Mercaptoacetic acid capped CdS quantum dots as fluorescence single shot probe for mercury(II), Sensors Actuators B Chem. 139 (2009) 91–96, https://doi.org/10.1016/j.snb.2008.09.011.
[44] J. Li, Y.-B. Wang, J.-D. Qiu, D.-c. Sun, X.-H. Xia, Biocomposites of covalently linked glucose oxidase on carbon nanotubes for glucose biosensor, Anal. Bioanal. Chem. 383 (2005) 918–922, https://doi.org/10.1007/s00216-005-0106-6.
[45] J. Shen, M. Shi, B. Yan, H. Ma, N. Li, Y. Hu, M. Ye, Covalent attaching protein to graphene oxide via diimide-activated amidation, Colloids Surf., B 81 (2010) 434–438, https://doi.org/10.1016/j.colsurfb.2010.07.035.
[46] H. Liu, H. Zhang, B. Jin, Fluorescence of tryptophan in aqueous solution, Spectrochim. Acta, Part A 106 (2013) 54–59, https://doi.org/10.1016/j.saa.2012.12.065.
[47] D.M. Togashi, B. Szczupak, A.G. Ryder, A. Calvet, M. O'Loughlin, Investigating Tryptophan Quenching of Fluorescein Fluorescence under Protolytic Equilibrium, J. Phys. Chem. A 113 (2009) 2757–2767, https://doi.org/10.1021/jp808121y.
[48] S. Roy, T.K. Das, Study of Interaction between Tryptophan, Tyrosine, and Phenylalanine separately with Silver Nanoparticles by Fluorescence Quenching Method, J. Appl. Spectrosc. 82 (2015) 598–606, https://doi.org/10.1007/s10812-015-0151-7.
[49] L. Bao, Z.-L. Zhang, Z.-Q. Tian, L. Zhang, C. Liu, Y. Lin, B. Qi, D.-W. Pang, Electrochemical Tuning of Luminescent Carbon Nanodots: from Preparation to Luminescence Mechanism, Adv. Mater. (Weinheim, Ger.) 23 (2011) 5801–5806, https://doi.org/10.1002/adma.201102866.
[50] N.J.B. Green, S.M. Pimblott, M. Tachiya, Generalizations of the Stern-Volmer relation, J. Phys. Chem. 97 (1993) 196–202, https://doi.org/10.1021/j100103a034.